Deep Gamblers: Learning to Abstain with Portfolio Theory

Liu Ziyin[†], **Zhikang T. Wang**[†], **Paul Pu Liang**[♭],
Ruslan Salakhutdinov[♭], **Louis-Philippe Morency**[◇], **Masahito Ueda**[†]
[†]Institute for Physics of Intelligence & Department of Physics, University of Tokyo
[♭]Machine Learning Department, Carnegie Mellon University
[◇]Language Technologies Institute, Carnegie Mellon University
{zliu,wang}@cat.phys.s.u-tokyo.ac.jp ueda@phys.s.u-tokyo.ac.jp
{pliang,rsalakhu,morency}@cs.cmu.edu

Abstract

We deal with the *selective classification* problem (supervised-learning problem with a rejection option), where we want to achieve the best performance at a certain level of coverage of the data. We transform the original m-class classification problem to $(m+1)$-class where the $(m+1)$-th class represents the model abstaining from making a prediction due to disconfidence. Inspired by portfolio theory, we propose a loss function for the selective classification problem based on the doubling rate of gambling. Minimizing this loss function corresponds naturally to maximizing the return of a *horse race*, where a player aims to balance between betting on an outcome (making a prediction) when confident and reserving one's winnings (abstaining) when not confident. This loss function allows us to train neural networks and characterize the disconfidence of prediction in an end-to-end fashion. In comparison with previous methods, our method requires almost no modification to the model inference algorithm or model architecture. Experiments show that our method can identify uncertainty in data points, and achieves strong results on SVHN and CIFAR10 at various coverages of the data.

1 Introduction

With deep learning's unprecedented success in fields such as image classification [21, 18, 24], language understanding [9, 35, 42, 32], and multimodal learning [26, 33], researchers have now begun to apply deep learning to facilitate scientific discovery in fields such as physics [2], biology [38], chemistry [16], and healthcare [20]. However, one important challenge for applications of deep learning to these natural science problems comes from the requirement of assessing the confidence level in prediction. Characterizing confidence and uncertainty of model predictions is now an active area of research [12], and being able to assess prediction confidence allows us to handpick difficult cases and treat them separately for better performance [13] (e.g., by passing to a human expert). Moreover, knowing uncertainty is important for fundamental machine learning research [19]; for example, many reinforcement learning algorithms (such as Thompson sampling [40]) requires estimating uncertainty of the distribution [39].

However, there has not been any well-established, effective and efficient method to assess prediction uncertainty of deep learning models. We believe that there are four desiderata for any framework to assess deep learning model uncertainty. Firstly, they must be *simply end-to-end trainable*, because end-to-end trainability is important for accessibility to the method. Secondly, it should require *no heavy sampling procedure* because sampling a model or prediction (as in Bayesian methods) hundreds of times is computationally heavy. Thirdly, it *should not require retraining* when different levels of uncertainty are required because many tasks such as ImageNet [8] and 1 Billion Word [4] require

33rd Conference on Neural Information Processing Systems (NeurIPS 2019), Vancouver, Canada.

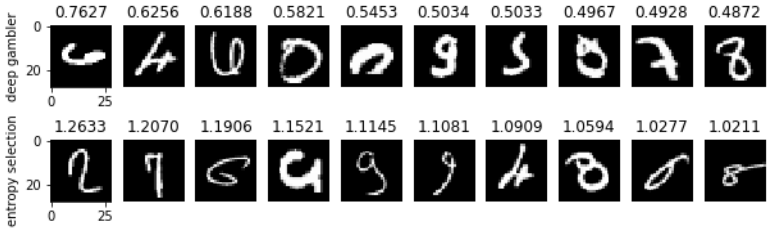

Figure 1: Top-10 rejected images in the MNIST testing set found by two methods. The number above image is the predicted uncertainty score (ours) or the entropy of the prediction (baseline). For the top-2 images, our method chooses images that are hard to recognize, while that of the baseline can be identified unambiguously by human.

weeks of training, which is too expensive. Lastly, it *should not require any modification to existing model architectures* so that we can achieve better flexibility and minimal engineering effort. However, most of the methods that currently exist do not meet some of the above criteria. For example, existing Bayesian approaches, in which priors of model parameters are defined and the posteriors are estimated using the Bayes theorem [29, 13, 34], usually rely heavily on sampling to estimate the posterior distribution [13, 34] or modifying the network architecture via the reparametrization trick [22, 3]. These methods therefore incur computational costs which slow down the training process. This argument also applied to ensembling methods [25]. Selective classification methods offer an alternative approach [5], which either require modifying model objectives and retraining the model [14, 15]. See Table 1 for a summary of the existing methods, and the problems with these methods are discussed in Section 3. In this paper, we follow the selective classification framework (see Section 2), and focus on a setting where we only have a single classifier augmented with a rejection option[1]. Inspired by portfolio theory in mathematical finance [30], we propose a loss function for the selective classification problem that is easy to optimize and requires almost no modification to existing architectures.

2 The Selective Prediction Problem

In this work, we consider a selective prediction problem setting [10]. Let X be the feature space and Y the label space. For example, X could be the distribution of images, and Y would be the distribution of the class labels, and our goal is to learn the conditional distribution $P(Y|X)$, and a *prediction model* parametrized by weight $\mathbf{w}$ is a function $f_{\mathbf{w}} : X \to Y$. The *risk* of the task w.r.t to a loss function $\ell(\cdot)$ is $\mathbb{E}_{P(X,Y)}[\ell(f(x), y)]$, given a dataset with size N $\{(x_i, y_i)\}_{i=1}^N$ where all (x_i, y_i) are independent draws from $X \times Y$. A prediction model augmented with a rejection option is a pair of functions (f, g) such that $g_h : X \to \mathbb{R}$ is a selection function which can be interpreted as a binary qualifier for f as follow:

$$(f, g)(x) := \begin{cases} f(x), & \text{if } g_h(x) \geq h \\ \text{ABSTAIN}, & \text{otherwise} \end{cases} \tag{1}$$

i.e., the model abstains from making a prediction when the selection function $g(x)$ falls below a predetermined threshold h. We call $g(x)$ the uncertainty score of x; different methods tend to use different $g(x)$. The *covered dataset* is defined to be $\{x : g_h(x) \geq h\}$, and the *coverage* is the ratio of the size of covered dataset to the size of the original dataset. Clearly, one may trade-off coverage for lower risk, and this is the motivation behind rejection option methods.

3 Related Work

Abstention Mechanisms. Here we summarize the existing methods to perform abstention, and these are the methods we will compare with in this paper. For a summary of the features of these methods, see table 1. **Entropy Selection (ES)**: This is the simplest way to output an uncertainty score for a prediction, we compare with this in the qualitative experiments. It simply takes the entropy of the predicted probability as the uncertainty score. **Softmax-Response (SR, [14])**: This is a simple yet theoretically-guaranteed strong baseline proposed in [14]. It regards the maximum predicted probability as the confidence score; it differs from our work in that it does not involve *training* an

[1] i.e., we do not consider ensembling methods, but we note that such method can be used together with our method and is likely to increase performance

	Ours	SR [14]	BD [13]	SN [15]
Simple end-to-end training	✓	✓	✓	✗
No sampling process required	✓	✓	✗	✓
No retraining needed for different coverage	✓	✓	✓	✗
No modification to model architecture	✓	✓	✓	✗

Table 1: Summary of features of different methods for selective prediction. Our method is end-to-end trainable and does not require sampling, retraining, or architecture modification.

abstention mechanism. **Bayes Dropout (BD, [13])**: This is a SOTA Bayesian method that offer a way to reject uncertain images [13]. One problem with with method is that one often needs about extensive sampling to obtain an accurate estimation of the uncertainty. **SelectiveNet (SN, [15])**: This is a very recent work that also trains a network to predict its uncertainty, and is the current SOTA method of the selective prediction problem. The loss function of this method requires interior point method to optimize and depends on the target coverage one wants to achieve.

Portfolio Theory and Gambling The Modern Portfolio Theory (MPT) is a modern method in investment for assembling a portfolio of assets that maximizes expected return while minimizing the risk [30]. The generalized portfolio theory is a constrained minimization problem in which we sought for maximum expected return with a variance constraint. In this work, however, we explore a very limited form of portfolio theory that can be seen as a *horse race*, as a proof of concept for bridging uncertainty in deep learning and portfolio theory. In this work, we focus on the classification problem, and we believe that regression problems can similarly be reformulated as a general portfolio problem, and we leave this line of research to the future. The connection between portfolio theory, gambling and information theory is studied in [6, 7]. Some of the theoretical arguments presented in this work are based on arguments given in [7].

4 Learning to Abstain with Portfolio Theory

The intuition behind the method is that a deep learning model learning to abstain from prediction indeed mimicks a gambler learning to reserve betting in a game. Indeed, we show that if we have a m-class classification problem, we can instead perform a $m+1$ class classification which predicts the probabilities of the m classes and use the $(m+1)$-th class as an additional rejection score. This method is similar to [14, 15], and the difference lies in how we learn such a model. We use ideas from portfolio theory which says that if we have some budget, we should split them between how much we would like to bet, and how much to save. In the following sections, we first provide a gentle introduction to portfolio theory which will provide the mathematical foundations of our method. We then describe how to adapt portfolio theory for classification problems in machine learning and derive our adapted loss function that trains a model to predict a rejection score. We finally prove some theoretical properties of our method to show that a classification problem can indeed be seen as a gambling problem, and thus avoiding a bet in gambling can indeed been interpreted as giving a rejection score.

4.1 A Short Introduction to General Portfolio Theory

To keep the terminology clear, we give a chart of the terms from portfolio theory and their corresponding concepts in deep learning in Table 2. The rows in the dictionary show the correspondences we are going to make in this section. In short, portfolio theory tells us what is the best way to invest in a stock market. A stock market with m stocks is a vector of positive real numbers $\mathbf{X} = (X_1, ..., X_m)$, and we define the *price relaive* X_i as the ratio of the price of the stock i at the end of the day to the price at the beginning of the day. For example, $X_i = 0.95$ means that the price of the stock is 0.95 times its price at the beginning of the day. We formulate the price vector as a vector of random variables drawn from a joint distribution $\mathbf{X} \sim P(\mathbf{X})$. A *portfolio* refers to our investment in this stock market, and can be modeled as a discrete distribution $\mathbf{b} = (b_1, ..., b_m)$ where $b_i \geq 0$ and $\sum_i b_i = 1$, and $\mathbf{b}$ is our distributing of wealth to $\mathbf{X}$. In this formulation, the *wealth relative* at the end of the day is $S = \mathbf{b}^T\mathbf{X} = \sum_i b_i X_i$; this tell us the ratio of our wealth at the end of the day to our wealth at the beginning of the day.

Portfolio Theory	Deep Learning
Portfolio	Prediction
Doubling Rate	negative NLL loss
Stock/Horse	input data point
Stock Market Outcome	Target Label
Horse Race Outcome	Target Label
Reservation in Gamble	Abstention

Table 2: Portfolio Theory - Deep Learning Dictionary.

Definition 1. *The doubling rate of a stock market portfolio* $\mathbf{b}$ *with respect to a stock distribution* $P(\mathbf{X})$ *is*

$$W(\mathbf{b}, P) = \int \log_2 \left(\mathbf{b}^T \mathbf{x} \right) dP(\mathbf{x}).$$

This tells us the speed at which our wealth increases, and we want to maximize W. Now we consider a simplified version of portfolio theory called the "horse race".

4.2 Horse Race

Different from a stock market, a horse race has an exclusive outcome (only one horse wins, and it's either win or loss) $\mathbf{x}(j) = (0, ..., 0, 1, 0, ..., 0)$, which is a one-hot vector on the j -th entry. In a horse race, we want to bet on m horses, and the i-th horse wins with probability p_i, and the payoff is o_i for betting 1 dollar on horse i if i wins, and the payoff is 0 otherwise. Now the gambler can choose to distribute his wealth over the m horses, according to $\mathbf{o}$ and $\mathbf{p}$, and let $\mathbf{b}$ denote such distribution; this corresponds to choosing a portfolio. Again, we require that $b_i \geq 0$, and $\sum_i b_i = 1$. The *wealth relative* of the gambler at the end of the game will be $S(\mathbf{x}(j)) = b_j o_j$ when the horse j wins. After n many races, our wealth relative would be:

$$S_n = \prod_{i=1}^{n} S(\mathbf{x}_i). \tag{2}$$

Notice that our relative wealth after n races does not depend on the order of the occurrence of the result of each race (and this will justify our treatment of a batch of samples as races). We can define the doubling rate by changing the integral to a sum:

Definition 2. *The doubling rate of a horse race is*

$$W(\mathbf{b}, \mathbf{p}) = \mathbb{E} \log_2(S) = \sum_{i=1}^{m} p_i \log_2(b_i o_i).$$

As before, we want to maximize the doubling rate. Notice that if we take $o_i = 1$ and b_i be the post-softmax output of our model, then W is equivalent to the commonly used cross-entropy loss in classification. However, a horse race can be more general because the gambler can choose to bet only with part of his money and reserve the rest to minimize risk. This means that, in a horse race with reservation, we can bet on $m + 1$ categories where the $m + 1$-th category denotes reservation with payoff 1. Now the wealth relative after a race becomes $S(\mathbf{x}_j) = b_j o_j + b_{m+1}$ and our objective becomes $\max_{\mathbf{b}} W(\mathbf{b}, \mathbf{p})$, where

$$\max W(\mathbf{b}, \mathbf{p}) = \sum_{i=1}^{m} p_i \log(b_i o_i + b_{m+1}). \tag{3}$$

This is the *gambler's loss*.

4.3 Classification as a Horse Race

An m-class classification task can be seen as finding a function $f : \mathbb{R}^n \to \mathbb{R}^m$, where n is the input dimension and m is the number of classes. For an output $f(x)$, we assume that it is normalized, and we treat the output of $f(\cdot)$ as the probability of input x being labeled in class j:

$$\Pr(j|x) = f(x)_j \tag{4}$$

Now, let us parametrize the function f as a neural network with parameter $\mathbf{w}$, whose output is a distribution over the class labels. We want to maximize the log probability of the true label j:

$$\max \mathbb{E}[\log p(j|x)] = \max_{\mathbf{w}} \mathbb{E}[\log f_{\mathbf{w}}(x)_j] \tag{5}$$

For a m-class classification task, we transform it to a horse race with reservation by adding a $m + 1$-th class, which stands for reservation. The objective function for a mini-batch of size B, and for constant o over all categories is then (cf. Equation 3)

$$\max_f W(\mathbf{b}(f), \mathbf{p}) = \max_{\mathbf{w}} \sum_{i}^{B} \log \left[f_{\mathbf{w}}(x_i)_{j(i)} o + f_{\mathbf{w}}(x_i)_{m+1} \right]. \tag{6}$$

where i is the index over the batch, and $j(i)$ is the label of the i-th data point. As previously remarked, if $o_j = 1$ for all j and $b_{m+1} = 0$, we recover the standard supervised classification task. Therefore o

becomes a hyperparameter, and a higher o encourages the network to be confident in inferring, and a low o makes it less confident. In the next section, we will show that the problem is only meaningful for $1 < o < m$. The selection function $g(\cdot)$ is then $f_{\mathbf{w}}(\cdot)_{m+1}$(cf. Equation 1), and prediction on different coverage can be achieved by simply calibrating the threshhold h on a validation set. Also notice that an advantage of our method over the current SOTA method [15] is that our loss function does not depend on the coverage.

5 Information Theoretic Analysis

In this section, we analyze our formulation theoretically to explain how our method works. In the first theorem, we show that for a *horce race* without reservation, its optimal solution exists. We then show that, in a setting (gambling with side information) that resembles an actual classification problem, the optimal solution also exists, and it is the same as the optimal solution we expect for a classification problem. The last theorem deals with the possible range of o for a horse race with reservation, followed by a discussion about we should choose the hyperparameter o.

In the problem setting, we considered a gambling problem that is probabilistic in nature. It corresponds to a horse race in which, the distribution of winning horses is drawn from a predetermined distribution $P(Y)$ and no other information besides the indices of the horse is given. In this case, we show that the optimal solution should be proportional to $P(Y)$ when no reservation is allowed.

Theorem 1. *The optimal doubling rate is given by*

$$W^*(p) = \sum_i p_i \log o_i - H(p). \tag{7}$$

where $H(p) = -\sum p \log p$ is the entropy of the distribution p, and this rate is achieved by proportional gambling $\mathbf{b}^* = p$.

This result shows the equivalence between a prediction problem and a gambling problem. In fact, trying to minimize the natural log loss for a classification task is the same as trying to maximize the doubling rate in a gambling problem. However, in practice, we are often in a horse race where some information about the horse is known. For example, in the “MNIST" horse race, one sees a picture, and want to guess its category, i.e., one has access to side information. In the next theorem, we show that in a gambling game with side information, the optimal gambling strategy is obtained by a prediction that maximizes the mutual information between the horse (image) and the outcome (label). This is a classical theorem that can be found in [7]. The proofs are given in the appendix.

Theorem 2. *Let W denote the doubling rate defined in Def. 2. For a horse race Y to which some side information X is given, the amount of increase ΔW is*

$$\Delta W = I(X;Y) = \sum_{x,y} p(x,y) \log \frac{p(x,y)}{p(x)p(y)}. \tag{8}$$

This shows that the increase in the doubling rate from knowing X is bounded by the mutual information between the two. This means that the neural network, during training, will have to maximize the mutual information between the prediction and the true label of the sample. This shows that an image classification problem is exactly equal to a horse race with side information. However, the next theorem makes our formulation different from a standard classification task and can be seen as a generalization of it. We show that, when reservation is allowed, the optimal strategy changes with o, the return of winning. Especially, for some range of o, only trivial solutions to the gambling problem exist. Since the tasks in this work only deals with situations in which o is uniform across categories, we assume o to be uniform for clarity.

Theorem 3. *Let m be the number of horses, and let W be defined as in Eq. 3, and let $o_i = o$ for all i; then if $o > m$, the optimal betting always have $b_{m+1} = 0$; if $o < 1$, then the optimal betting always have $b_i = 0$ for $i \neq m + 1$.*

This theorem tells us that when the return from betting is too high ($o > m$), then we should always bet, and so the optimal solution is given by Theorem 1; when the return from betting is too low ($o < 1$), then we should always reserve. A more realistic situation should have that $1 < o < m$, which reflects the fact that, while one might expect to gain in a horse race, the organizer of the game takes a cut of the bets. We discuss the effect of varying o in the appendix (section 11.1). In fact, the optimal rejection score of to a given prediction probability of our method can be easily found

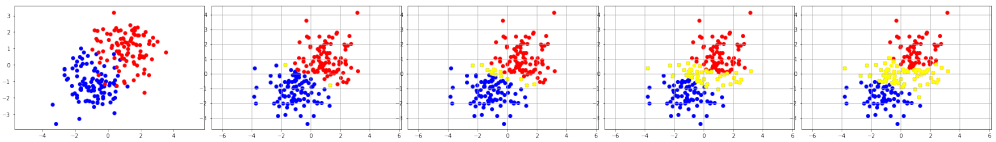

(a) Training Set (b) $h = 0.999$ (c) $h = 0.99$ (d) $h = 0.9$ (e) $h = 0.5$

Figure 2: Output of the network. h is the threshold, and yellow points are rejected points at this level of h.

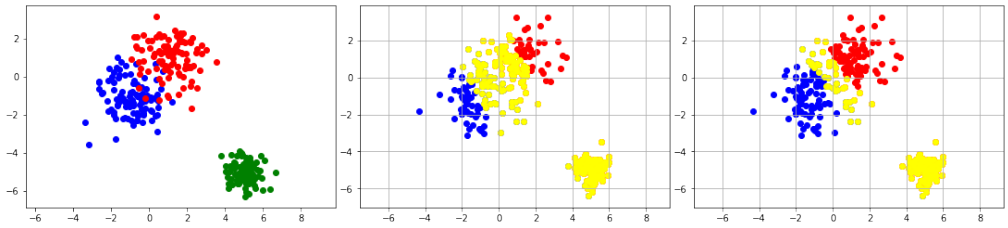

(a) Testing Set (b) entropy based (c) deep gamblers

Figure 3: Identifying the outlier distribution. h is chosen to be the largest value such that the outlier cluster is rejected. We see that a network trainied with our method rejects the outlier cluster much earlier than the entropy based method.

using Kuhn-Tucker condition without training the network, but we argue that it is not the learned rejection score that is the core of method, but that this loss function allows the trained model to learn a qualitatively different and better hidden representation than the baseline model. See Figure 5 (and appendix).

6 Experiments

We begin with some toy experiments to demonstrate that our method can deal with various kinds of uncertain inputs. We then compare the existing methods in selective classification and show that the proposed method is very competitive against the SOTA method. Implementation details are in the appendix.

6.1 Synthetic Gaussian Dataset

In this section, we train a network with 2 hidden layers each with 50 neurons and $tanh$ activation. For the training set, we generate 2 overlapping diagonal $2d$-Gaussian distributions and the task is a simple binary classification. Cluster 1 has mean $(1, 1)$ and unit variance, and cluster 2 has mean $(-1, -1)$ with unit variance. The fact that these two clusters are not linearly separable is the first source of uncertainty. A third out-of-distribution cluster exists only in the testing set to study how the model deals with out-of-distribution samples. This distribution has mean $(5, -5)$ and variance 0.5. This is the second source of uncertainty. Figure 2(a) shows the training set and 3(a) shows the test set.

We gradually decrease the threshold h for the predicted disconfident score, and label the points above the threshold as rejected. These results are visualized in Figure 2 and we observe that the model correctly identifies the border of the two Gaussian distributions as the uncertain region. We also see that, by lowering the threshold, the width of the uncertain region increases. This shows how we might calibrate threshold h to control coverage. Now we study how the model deals with out-of-distribution uncertainty. From Figure 3, we see that the entropy based selection is only able to reject the third cluster when most of data points are excluded, while our method seems to reject the outliers equally well with the boundary points.

6.2 Locating the outlier testing images of MNIST

In this section, we show the images that our method finds the most disconfident in MNIST in comparison with the entropy selection method in Figure 1. The model is a simple 4-layer CNN. We find that our method seems to outperform the baseline qualitatively. For example, the two least certain images found by the entropy based method can be labeled by a human unambiguously as a 2 and 7, while the top-2 images found by our method do not look like images of numbers at all. Most figures of this experiment and plots of how the images change across different epochs can be found in the appendix.

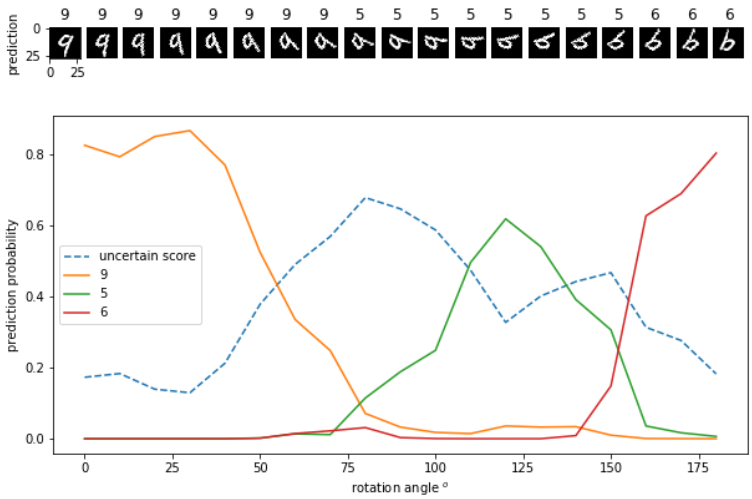

Figure 4: Rotating an image of 9 by 180 degrees. The number above the images are the prediction label of the rotated image.

Coverage	Ours (Best Single Model)	Ours (Best per coverage)	SR	BD	SN
1.00	$^{o=2.6}3.24 \pm 0.09$	–	3.21	3.21	3.21
0.95	$^{o=2.6}\mathbf{1.36 \pm 0.02}$	$^{o=2.6}\mathbf{1.36 \pm 0.02}$	1.39	1.40	1.40
0.90	$^{o=2.6}\mathbf{0.76 \pm 0.05}$	$^{o=2.6}\mathbf{0.76 \pm 0.05}$	0.89	0.90	0.82 ± 0.01
0.85	$^{o=2.6}\mathbf{0.57 \pm 0.07}$	$^{o=3.6}0.66 \pm 0.01$	0.70	0.71	$\mathbf{0.60 \pm 0.01}$
0.80	$^{o=2.6}\mathbf{0.51 \pm 0.05}$	$^{o=3.6}\mathbf{0.53 \pm 0.04}$	0.61	0.61	$\mathbf{0.53 \pm 0.01}$

Table 3: SVHN. The number is error percentage on the covered dataset; the lower the better. We see that our method achieved competitive results across all coverages. It is the SOTA method at coverage $(0.85, 1.00)$.

6.3 Rotating an MNIST image

For illustration, we choose an image of 9 and rotate it up to 180 degrees because a number 9 looks like a distorted 5 when rotated by 90 degrees and looks like a 6 when rotated by 180, which allows us to analyze the behavior of the model clearly. See figure 4. We see that the model assesses its disconfidence as we expected, labeling the image as 9 at the beginning and 6 at the end, and as a 5 with high uncertainty in an intermediate region. We also notice that the uncertainty score has two peaks corresponding to crossing of decision boundaries. This suggests that the model has really learned to assess uncertainty in a subtle and meaningful way (also see Figure 5).

6.4 Comparison with Existing Methods

In this section, we compare with the SOTA methods in selective classification. The experiment is performed on SVHN [31] (Table 3), CIFAR10 [23] (Table 4) and Cat vs. Dog (Table 5). We follow exactly the experimental setting in [15] to allow for fair comparison. We use a version of VGG16 that is especially optimized for small datasets [27] with batchnorm and dropout. The baselines we compare against are given in Section 3 and summarized in Table 1. A grid search is done over hyperparameter o with a step size of 0.2. The best models of ours for a given coverage are chosen using a validation set, which is separated from the test set by a fixed random seed, and the best single model is chosen by using the model that achieves overall best validation accuracy. To report error bars, we estimate its standard deviation using the test errors on neighbouring 3 hyperparameter o values in our grid search (e.g. for $o = 6.5$, the results from $o = 6.3, 6.5, 6.7$ are used to compute the variance).

The results for the baselines are cited from [15], and we show the error bar for the contender models when it overlaps or seem to overlap with our confidence interval. We see that our model achieves SOTA on SVHN on all coverages, in the sense that our model starts at full coverage with a slightly lower accuracy but starts to outperform other contenders starting from 0.95 coverage, meaning that it learned to identify the hard images better than its contenders. We also perform the experiment on CIFAR-10 and Cat vs. Dog datasets, and we see that our method achieves very strong results. A small problem for the comparison remains since our models have different full coverage performance

Coverage	Ours (Single Best Model)	Ours (Best per Coverage)	SR	BD	SN
1.00	$^{o=2.2}6.12 \pm 0.09$	–	6.79	6.79	6.79
0.95	$^{o=2.2}\mathbf{3.49 \pm 0.15}$	$^{o=6.0}3.76 \pm 0.12$	4.55	4.58	4.16
0.90	$^{o=2.2}\mathbf{2.19 \pm 0.12}$	$^{o=6.0}2.29 \pm 0.11$	2.89	2.92	2.43
0.85	$^{o=2.2}\mathbf{1.09 \pm 0.15}$	$^{o=2.0}1.24 \pm 0.15$	1.78	1.82	1.43
0.80	$^{o=2.2}\mathbf{0.66 \pm 0.11}$	$^{o=2.2}\mathbf{0.66 \pm 0.11}$	1.05	1.08	0.86
0.75	$^{o=2.2}\mathbf{0.52 \pm 0.03}$	$^{o=2.2}\mathbf{0.52 \pm 0.03}$	0.63	0.66	$\mathbf{0.48 \pm 0.02}$
0.70	$^{o=2.2}0.43 \pm 0.07$	$^{o=2.2}0.43 \pm 0.07$	0.42	0.43	$\mathbf{0.32 \pm 0.01}$

Table 4: CIFAR10. The number is error percentage on the covered dataset; the lower the better. We see that the superior performance of our method is seen again for another dataset.

Coverage	Ours (Single Best Model)	Ours (Best per Coverage)	SR	BD	SN
1.00	$^{o=2.0}2.93 \pm 0.17$	–	3.58	3.58	3.58
0.95	$^{o=2.0}1.23 \pm 0.12$	$^{o=1.4}\mathbf{0.88 \pm 0.38}$	1.91	1.92	1.62
0.90	$^{o=2.0}\mathbf{0.59 \pm 0.13}$	$^{o=2.0}\mathbf{0.59 \pm 0.13}$	1.10	1.10	0.93
0.85	$^{o=2.0}0.47 \pm 0.10$	$^{o=1.2}\mathbf{0.24 \pm 0.10}$	0.82	0.78	0.56
0.80	$^{o=2.0}\mathbf{0.46 \pm 0.08}$	$^{o=2.0}\mathbf{0.46 \pm 0.08}$	0.68	0.55	$\mathbf{0.35 \pm 0.09}$

Table 5: Cats vs. Dogs. The number is error percentage on the covered dataset; the lower the better. This dataset is a binary classification, and the input images have larger resolution.

from other methods, but a closer look suggests that our method performs indeed better when the coverage is in the range $[0.8, 1.0)$ (by comparing the relative improvements). Below 0.8 coverage, the comparison becomes hard since there are only few images remaining, and methods on different dataset show misleading performance: on Cats vs. Dogs for 0.8 coverage, statistical fluctuation caused the validated best model to be one of the worst models on test set.

7 Discussion and Conclusion

In this work, we have proposed an end-to-end method to augment the standard supervised classification problem with a rejection option. The proposed method works competitively against the current SOTA [15] but is simpler and more flexible, while outperforming the runner-up SOTA model [14]. We hypothesize that this is because that our model has learned a qualitatively better hidden representation of the data. In Figure 5, we plot the t-SNE plots of a regular model and a model trained with our loss function (more plots in Appendix). We see that, for the baseline, 6 of the clusters of the hidden representation are not easily separable (circled clusters), while a deep gambler model learned a representation with a large margin, which is often associated with superior performance [11, 28, 17].

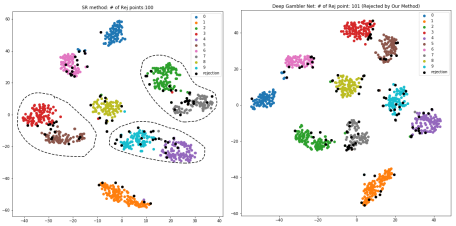

(a) Normal Model (b) Deep Gambler

Figure 5: t-SNE plot of the second-to-last layer output of a baseline and a deep gambler model for MNIST. Best viewed in color and zoomed-in. The deep gambler model learned a representation that is more separable.

It seems that there are many possible future directions this work might lead to. One possibility is to use it in scientific fields. For example, neural networks have been used in the classifying neutrinos, and if we do classification on a subset of the data but with higher confidence level, then we can better bound the frequency of neutrino oscillation, which is an important frontier in physics that will help us understand the fundamental laws of the universe [1]. This methods also seems to offer a way to interpret how a deep learning model learns. We can show the top rejected data points at different epochs to study what are the problems that the model finds difficult at different stages of training. Two other areas our method might also turn out to be helpful are robustness against adversarial attacks [37] and learning in the presence of label noise [36, 41]. This work also gives a way incorporate ideas from portfolio theory to deep learning. We hope this work will inspire further research in this direction.

Acknowledgements: Liu Ziyin thanks Mr. Zongping Gong for buying him drink sometimes, during the writing of this paper; he also thanks the GSSS scholarship at the University of Tokyo for supporting his graduate study. Z. T. Wang is supported by Global Science Graduate Course (GSGC) program of the University of Tokyo. This material is based upon work partially supported by the National Science Foundation (Awards $\#1734868, \#1722822$) and National Institutes of Health. Any opinions, findings, and conclusions or recommendations expressed in this material are those of the author(s) and do not necessarily reflect the views of National Science Foundation or National Institutes of Health, and no official endorsement should be inferred. Also, This work was supported by KAKENHI Grant No. JP18H01145 and a Grant-in-Aid for Scientific Research on Innovative Areas "Topological Materials Science" (KAKENHI Grant No. JP15H05855) from the Japan Society for the Promotion of Science.

References

[1] K. Abe, Y. Hayato, T. Iida, K. Iyogi, J. Kameda, Y. Koshio, Y. Kozuma, Ll. Marti, M. Miura, S. Moriyama, M. Nakahata, S. Nakayama, Y. Obayashi, H. Sekiya, M. Shiozawa, Y. Suzuki, A. Takeda, Y. Takenaga, K. Ueno, K. Ueshima, S. Yamada, T. Yokozawa, C. Ishihara, H. Kaji, T. Kajita, K. Kaneyuki, K. P. Lee, T. McLachlan, K. Okumura, Y. Shimizu, N. Tanimoto, L. Labarga, E. Kearns, M. Litos, J. L. Raaf, J. L. Stone, L. R. Sulak, M. Goldhaber, K. Bays, W. R. Kropp, S. Mine, C. Regis, A. Renshaw, M. B. Smy, H. W. Sobel, K. S. Ganezer, J. Hill, W. E. Keig, J. S. Jang, J. Y. Kim, I. T. Lim, J. B. Albert, K. Scholberg, C. W. Walter, R. Wendell, T. M. Wongjirad, T. Ishizuka, S. Tasaka, J. G. Learned, S. Matsuno, S. N. Smith, T. Hasegawa, T. Ishida, T. Ishii, T. Kobayashi, T. Nakadaira, K. Nakamura, K. Nishikawa, Y. Oyama, K. Sakashita, T. Sekiguchi, T. Tsukamoto, A. T. Suzuki, Y. Takeuchi, M. Ikeda, A. Minamino, T. Nakaya, Y. Fukuda, Y. Itow, G. Mitsuka, T. Tanaka, C. K. Jung, G. D. Lopez, I. Taylor, C. Yanagisawa, H. Ishino, A. Kibayashi, S. Mino, T. Mori, M. Sakuda, H. Toyota, Y. Kuno, M. Yoshida, S. B. Kim, B. S. Yang, H. Okazawa, Y. Choi, K. Nishijima, M. Koshiba, M. Yokoyama, Y. Totsuka, K. Martens, J. Schuemann, M. R. Vagins, S. Chen, Y. Heng, Z. Yang, H. Zhang, D. Kielczewska, P. Mijakowski, K. Connolly, M. Dziomba, E. Thrane, and R. J. Wilkes. Evidence for the appearance of atmospheric tau neutrinos in super-kamiokande. *Phys. Rev. Lett.*, 110:181802, May 2013.

[2] Pierre Baldi, Peter Sadowski, and Daniel Whiteson. Searching for exotic particles in high-energy physics with deep learning. *Nature communications*, 5:4308, 2014.

[3] Charles Blundell, Julien Cornebise, Koray Kavukcuoglu, and Daan Wierstra. Weight uncertainty in neural networks. *arXiv preprint arXiv:1505.05424*, 2015.

[4] Ciprian Chelba, Tomas Mikolov, Mike Schuster, Qi Ge, Thorsten Brants, Phillipp Koehn, and Tony Robinson. One billion word benchmark for measuring progress in statistical language modeling. *arXiv preprint arXiv:1312.3005*, 2013.

[5] Chi-Keung Chow. An optimum character recognition system using decision functions. *IRE Transactions on Electronic Computers*, (4):247–254, 1957.

[6] Thomas M. Cover. Universal portfolios. *Mathematical Finance*, 1(1):1–29, 1991.

[7] Thomas M. Cover and Joy A. Thomas. *Elements of Information Theory (Wiley Series in Telecommunications and Signal Processing)*. Wiley-Interscience, New York, NY, USA, 2006.

[8] Jia Deng, Wei Dong, Richard Socher, Li jia Li, Kai Li, and Li Fei-fei. Imagenet: A large-scale hierarchical image database. In *In CVPR*, 2009.

[9] Jacob Devlin, Ming-Wei Chang, Kenton Lee, and Kristina Toutanova. BERT: pre-training of deep bidirectional transformers for language understanding. *CoRR*, abs/1810.04805, 2018.

[10] Ran El-Yaniv and Yair Wiener. On the foundations of noise-free selective classification. *Journal of Machine Learning Research*, 11(May):1605–1641, 2010.

[11] Gamaleldin Elsayed, Dilip Krishnan, Hossein Mobahi, Kevin Regan, and Samy Bengio. Large margin deep networks for classification. In *Advances in Neural Information Processing Systems*, pages 842–852, 2018.

[12] Yarin Gal. Uncertainty in deep learning. 2016.

[13] Yarin Gal and Zoubin Ghahramani. Dropout as a Bayesian Approximation: Representing Model Uncertainty in Deep Learning. *arXiv e-prints*, page arXiv:1506.02142, June 2015.

[14] Yonatan Geifman and Ran El-Yaniv. Selective classification for deep neural networks. In *Advances in neural information processing systems*, pages 4878–4887, 2017.

[15] Yonatan Geifman and Ran El-Yaniv. Selectivenet: A deep neural network with an integrated reject option. *arXiv preprint arXiv:1901.09192*, 2019.

[16] Garrett B Goh, Nathan O Hodas, and Abhinav Vishnu. Deep learning for computational chemistry. *Journal of computational chemistry*, 38(16):1291–1307, 2017.

[17] Trevor Hastie, Robert Tibshirani, and Jerome Friedman. *The Elements of Statistical Learning*. Springer Series in Statistics. Springer New York Inc., New York, NY, USA, 2001.

[18] Kaiming He, Xiangyu Zhang, Shaoqing Ren, and Jian Sun. Deep residual learning for image recognition. *CoRR*, abs/1512.03385, 2015.

[19] Yotam Hechtlinger, Barnabás Póczos, and Larry Wasserman. Cautious deep learning. *arXiv preprint arXiv:1805.09460*, 2018.

[20] Geoffrey Hinton. Deep learning—a technology with the potential to transform health care. *Jama*, 320(11):1101–1102, 2018.

[21] Gao Huang, Zhuang Liu, and Kilian Q. Weinberger. Densely connected convolutional networks. *CoRR*, abs/1608.06993, 2016.

[22] Diederik P Kingma and Max Welling. Auto-encoding variational bayes. *arXiv preprint arXiv:1312.6114*, 2013.

[23] Alex Krizhevsky, Vinod Nair, and Geoffrey Hinton. Cifar-10 (canadian institute for advanced research).

[24] Alex Krizhevsky, Ilya Sutskever, and Geoffrey E Hinton. Imagenet classification with deep convolutional neural networks. In F. Pereira, C. J. C. Burges, L. Bottou, and K. Q. Weinberger, editors, *Advances in Neural Information Processing Systems 25*, pages 1097–1105. Curran Associates, Inc., 2012.

[25] Balaji Lakshminarayanan, Alexander Pritzel, and Charles Blundell. Simple and scalable predictive uncertainty estimation using deep ensembles. In *Advances in Neural Information Processing Systems*, pages 6402–6413, 2017.

[26] Paul Pu Liang, Ziyin Liu, Amir Zadeh, and Louis-Philippe Morency. Multimodal language analysis with recurrent multistage fusion. *arXiv preprint arXiv:1808.03920*, 2018.

[27] Shuying Liu and Weihong Deng. Very deep convolutional neural network based image classification using small training sample size. In *2015 3rd IAPR Asian conference on pattern recognition (ACPR)*, pages 730–734. IEEE, 2015.

[28] Weiyang Liu. Large-margin softmax loss for convolutional neural networks.

[29] David JC MacKay. A practical bayesian framework for backpropagation networks. *Neural computation*, 4(3):448–472, 1992.

[30] Harry Markowitz. Portfolio selection. *The Journal of Finance*, 7(1):77–91, 1952.

[31] Yuval Netzer, Tao Wang, Adam Coates, Alessandro Bissacco, Bo Wu, and Andrew Y. Ng. Reading digits in natural images with unsupervised feature learning. In *NIPS Workshop on Deep Learning and Unsupervised Feature Learning 2011*, 2011.

[32] Graham Neubig. Neural machine translation and sequence-to-sequence models: A tutorial. *arXiv preprint arXiv:1703.01619*, 2017.

[33] Jiquan Ngiam, Aditya Khosla, Mingyu Kim, Juhan Nam, Honglak Lee, and Andrew Y Ng. Multimodal deep learning. In *Proceedings of the 28th international conference on machine learning (ICML-11)*, pages 689–696, 2011.

[34] Tim Pearce, Mohamed Zaki, Alexandra Brintrup, and Andy Neel. Uncertainty in neural networks: Bayesian ensembling. *arXiv preprint arXiv:1810.05546*, 2018.

[35] Alec Radford, Jeff Wu, Rewon Child, David Luan, Dario Amodei, and Ilya Sutskever. Language models are unsupervised multitask learners. 2019.

[36] David Rolnick, Andreas Veit, Serge Belongie, and Nir Shavit. Deep learning is robust to massive label noise. *arXiv preprint arXiv:1705.10694*, 2017.

[37] Andrew Slavin Ross and Finale Doshi-Velez. Improving the adversarial robustness and interpretability of deep neural networks by regularizing their input gradients. In *Thirty-second AAAI conference on artificial intelligence*, 2018.

[38] João Sacramento, Rui Ponte Costa, Yoshua Bengio, and Walter Senn. Dendritic cortical microcircuits approximate the backpropagation algorithm. In S. Bengio, H. Wallach, H. Larochelle, K. Grauman, N. Cesa-Bianchi, and R. Garnett, editors, *Advances in Neural Information Processing Systems 31*, pages 8721–8732. Curran Associates, Inc., 2018.

[39] Csaba Szepesvári. Algorithms for reinforcement learning. 2009.

[40] William R Thompson. On the likelihood that one unknown probability exceeds another in view of the evidence of two samples. *Biometrika*, 25(3/4):285–294, 1933.

[41] Arash Vahdat. Toward robustness against label noise in training deep discriminative neural networks. In *Advances in Neural Information Processing Systems*, pages 5596–5605, 2017.

[42] Ashish Vaswani, Noam Shazeer, Niki Parmar, Jakob Uszkoreit, Llion Jones, Aidan N. Gomez, Lukasz Kaiser, and Illia Polosukhin. Attention is all you need. *CoRR*, abs/1706.03762, 2017.

Appendix

8 A practitioner's guide to our method

8.1 Implementation

We give a summary of our proposed method here such that the method can be implemented only reading this section. For a m-class classification problem, we propose to change the cross entropy loss to the following modified one:

$$\sum_{i=1}^{m} p_i \log(\hat{p}_i) \to \sum_{i=1}^{m} p_i \log(\hat{p}_i + \frac{1}{o}\hat{p}_{m+1}) \tag{9}$$

where $\hat{p}_i$ denotes the output prediction of the model for label i, and the constraint $\sum_{i=1}^{m+1} \hat{p}_i = 1$ is explicitly enforced by a softmax function over the pre-softmax values; o is a hyperparameter that one can tune, which should be equal to or smaller than m but larger than 1. $\hat{p}_{m+1}$ is the augmented rejection score predicted by the model. For neural networks, this amounts to changing the output dimension from m to $m+1$, and using the loss function above to train the rejection score p_{m+1}. All other settings of training may be kept the same. The gambler's loss can be written in Pytorch as the following lines:

```
def gambler_loss(model_output, targets):
    outputs = torch.nn.functional.softmax(model_output, dim=1)
    outputs, reservation = outputs[:,:-1], outputs[:,-1]
    gain = torch.gather(outputs, dim=1, index=targets.unsqueeze(1)) \
                                                        .squeeze()
    doubling_rate = (gain+reservation/reward).log()
    return -doubling_rate.mean()
```

8.2 Optimizing the deep gambler's Objective

When training the neural network models, we experimentally found that if o is overly small, the neural network sometimes fails to learn from the training data and converges to a trivial point, which only predicts to abstain, especially on more difficult datasets such as CIFAR10. On CIFAR10, in our grid search experiments, when $o < 6.3$ the trained neural network converged trivially, and when $o \geq 6.3$ the trained model performed at least as well as the ones trained in usual ways. Therefore, in order to converge non-trivially with $o < 6.3$ values, it can be trained with usual cross entropy loss for several epochs in the beginning, and changed to our proposed loss later. This training schedule works well and produces prediction accuracy comparable to large o values. On dataset CIFAR 10, we trained our model with usual cross entropy loss for the first 100 epochs when $o < 6.3$; on dataset SVHN, we trained with cross entropy for the first 50 epochs when $o < 6.0$; on dataset Cats vs Dogs, we trained with cross entropy for the first 50 epochs for all o values.

9 Theorem Proofs

Theorem. *The optimal doubling rate is given by:*

$$W^*(\mathbf{p}) = \sum p_i \log o_i - H(p) \tag{10}$$

where $H(p) = -\sum p \log p$ is the entropy of the distribution p, and this rate is achieved by proportional gambling $\mathbf{b}^* = p$.

Proof. we have

$$\begin{aligned} W(\mathbf{b}, \mathbf{p}) &= \sum_i p_i \log(b_i o_i) \\ &= -H(\mathbf{p}) - D(\mathbf{p}||\mathbf{b}) + \sum_i p_i \log o_i \\ &\leq \sum_i p_i \log o_i - H(\mathbf{p}) \end{aligned}$$

and the equality only holds when $\mathbf{b} = \mathbf{p}$.

Theorem. *Let W denote the doubling rate given in Def. 2. For a horse race X to which some side information Y is given, the increase ΔW is:*

$$\Delta W = I(X;Y) = \sum_{x,y} p(x,y) \log \frac{p(x,y)}{p(x)p(y)}. \tag{11}$$

Proof. Simply modifying the proof above, it is easy to show that the optimal gambling strategy with side information Y is obtained also by proportional gambling $b(x|y) = p(x|y)$. By definition:

$$\begin{aligned} W^*(X|Y) &= \max_{\mathbf{b}(x|y)} \sum p(x,y) \log(o(x)b(x|y)) \\ &= \sum p(x,y) \log(o(x)p(x|y)) \\ &= -H(X|Y) + \sum p(x) \log o(x) \end{aligned}$$

comparing with the doubling rate without side information, we see that the change in doubling rate is:

$$\Delta W = W^*(X|Y) - W^*(X) = H(X) - H(X|Y) = I(X;Y)$$

and we are done.

Theorem. *Let m be the number of horses, and let the W be defined as in Eq. 3, and let $o_i = o$ for all i, then if $o \geq m$, then the optimal betting always have $b_{m+1} = 0$; if $0 \leq 1$, then the optimal betting always have $b_{m+1} = ||\mathbf{b}||_1$.*

Proof. (1) We first consider the case $o < 1$, we want to show that the optimal solution is to always reserve (i.e. $b_i = 0$ for $i \in \{1, ..., m\}$). Suppose that there exist a solution where $b_i \neq 0$, then the expected return of this part of the bet is then $o_i p_i b_i$, since $p_i \leq 1$, $p_i o_i b_i < 1 = b_i$. This shows that if we instead distribute b_i percentage of our wealth to b_{m+1}, then we will achieve better result.

(2) Now we show that for the case $o > m$, we should have $b_{m+1} = 0$. Again, we adopt similar strategy by showing that if there is a solution for which $b_{m+1} \neq 0$, then we can always find a solution better than this. Let $b_{m+1} \neq 0$, and we compare this with a solution in which we distribute b_{m+1} evenly to categories 1 to m, the difference in return is:

$$\sum_{i=1}^{m} \frac{p_i b_{m+1} o}{m} - b_{m+1} = \frac{b_{m+1} o}{m} \sum_{i=1}^{m} p_i - b_{m+1} = b_{m+1} \frac{o}{m} - b_{m+1} > 0$$

since $b_{m+1} > m$, and we are done.

10 Experiment Detail

For all of our experiments, we use the PyTorch framework[2]. The version is 1.0. We will release the code of our paper at http://********.

10.1 Datasets

Street View House Numbers (SVHN). The SVHN dataset is an image classification dataset containing $73,257$ training images and $26,032$ test images divided into 10 classes. The images are digits of house street numbers. Image size is $32 \times 32 \times 3$ pixels. We use the official dataset downloaded by Pytorch utilities.

CIFAR-10. The CIFAR10 dataset is an image classification dataset comprising a training set of $50,000$ training images and $10,000$ test images divided into 10 categories. The image size is $32 \times 32 \times 3$ pixels. We use the official dataset downloaded by Pytorch.

Cats vs. Dogs. The Cats vs. Dogs dataset is an image binary classification dataset comprising a set of $25,000$ images[3]. As in [15], we randomly choose $20,000$ images as training set and 5000 images as testing set. We resize the size of the images to $64 \times 64 \times 3$.

[2] `https://pytorch.org/`

[3] `https://www.kaggle.com/c/dogs-vs-cats/overview`

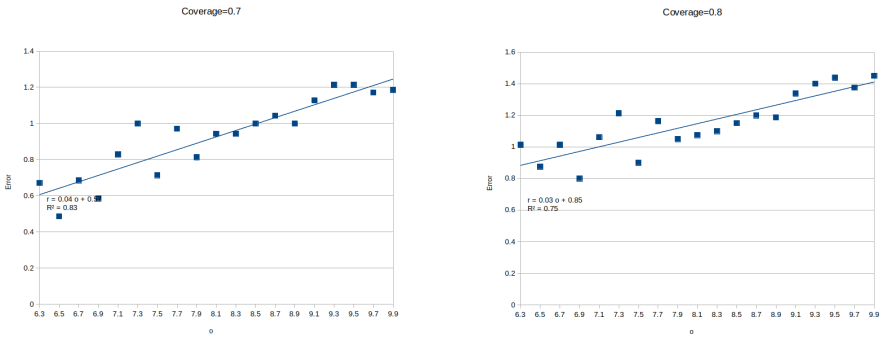

Figure 6: Error on CIFAR-10 for coverage 0.7 and 0.8 for different o. o values below this region require cross entropy loss pretraining to proceed normally, and the results deviate from the above trend lines.

10.2 Experiment Setting Details

We follow exactly the experiment setting in [15] and the details are checked against the open source code in [15]. The grid search is done over hyperparameter o with a step size of 0.2, and the best models of ours for a given coverage are chosen using a validation set. The grid search of o is from 2 to 9.8 on CIFAR-10, from 2 to 8 on SVHN, and from 1.2 to 2 on Cats vs. Dogs. The validation set sizes for SVHN, CIFAR-10 and Cats vs. Dogs are respectively 5000, 2000 and 2000. The standard deviations are estimated by test errors on neighbouring 3 hyperparameter o values in the grid search.[4]

11 Additional Experimental Results

11.1 Tuning the hyperparameter

The only hyperparameter we introduced is o, of which a larger value encourages the model to be less reserved. In this section, we show that o is correlated to the performance of the model at a given coverage and thus is a very meaningful parameter. See figure 6. We see that a lower o causes the model to learn to reject better, but with a larger variance. This suggests that tuning o for different tasks and needs is beneficial. Especially, when o is close to 1, the trained model does not converge to a small training error, and this training error is comparable to its test error. In this case, its resultant total test error rate is increased. However, when o is large, the model does not learn to perform well at low coverages, because the trained abstention score is overly small and affected by numerical error. Therefore, there is a trade-off between total error and error at low coverages, and tuning o is indeed meaningful. Moreover, an appropriate o value encourages the model to learn more from its certain data and learn less from its uncertain data, when compared to the usual cross entropy loss. We believe this is the reason that many of our validated best models outperform the accuracy of the baseline models that use cross entropy loss, even when we train exactly the same models using the same Pytorch package. Therefore, in most situations the best performance is achieved when o is either small or large.

11.2 Top-30 Least Certain Images

Here we plot top-30 least certain images in the MNIST training set identified by a trained 4-layer CNN using our method. We also show that how this list changes at epoch $1, 10, 30$. By doing this, we can understand what are the images that the network finds the hardest to identify at different stages of training. We note that the model converges at about 10 epoch.

[4]The code to this work is available at:
`https://github.com/Z-T-WANG/NIPS2019DeepGamblers`

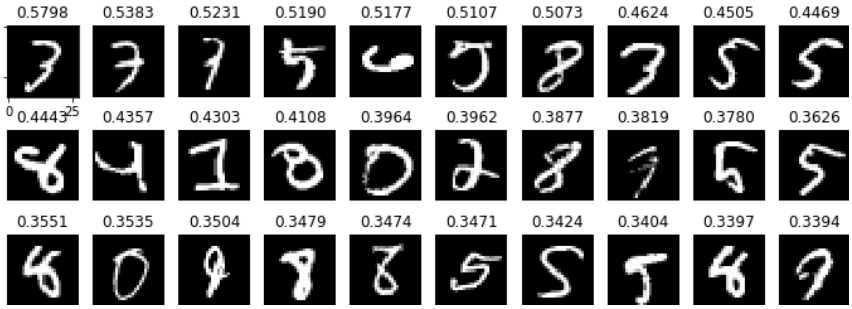

Figure 7: Epoch 1. The top-30 images in the MNIST testing set found by Deep Gamblers, with the uncertainty score at the top.

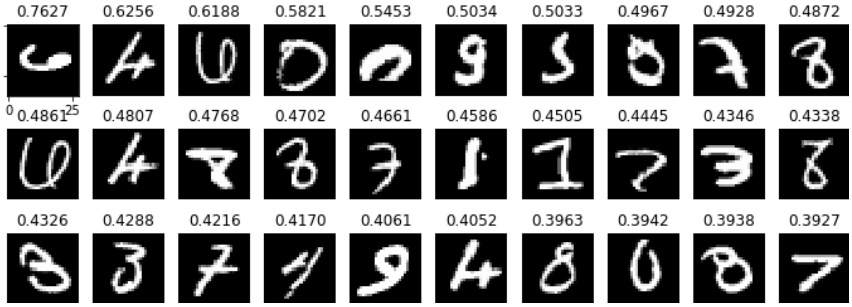

Figure 8: Epoch 10. The top-30 images in the MNIST testing set found by Deep Gamblers, with the uncertainty score at the top.

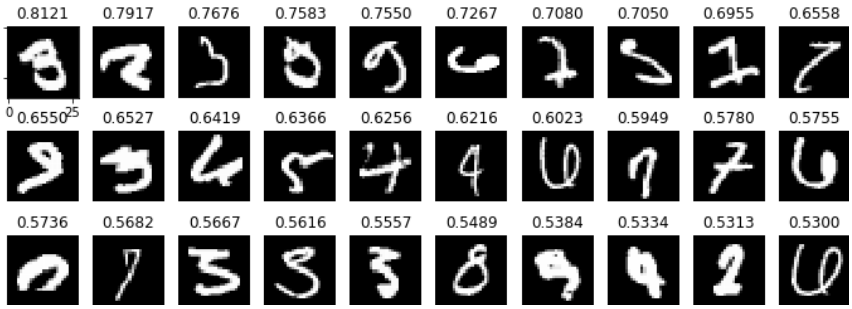

Figure 9: Epoch 30. The top-30 images in the MNIST testing set found by Deep Gamblers, with the uncertainty score at the top.

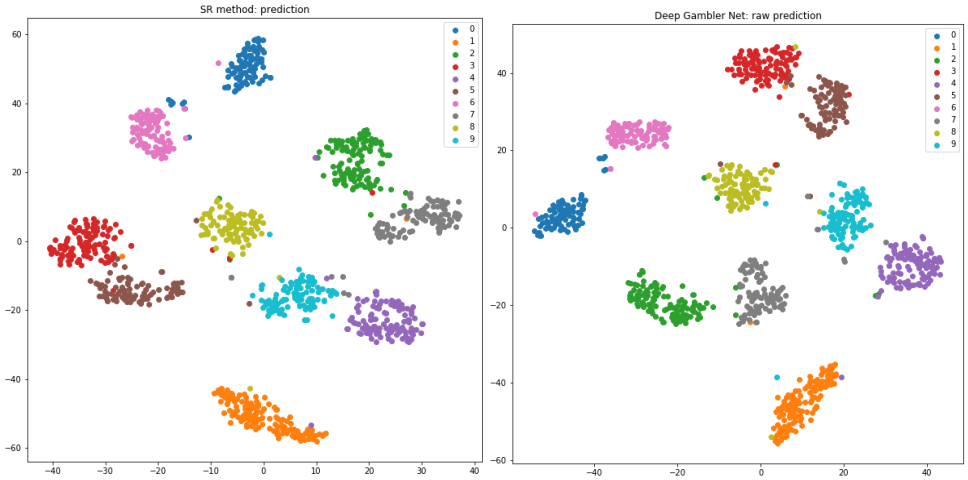

(a) Normal Model (b) Deep Gambler

Figure 10: t-SNE plot of a normal model and the same model trained using our loss function.

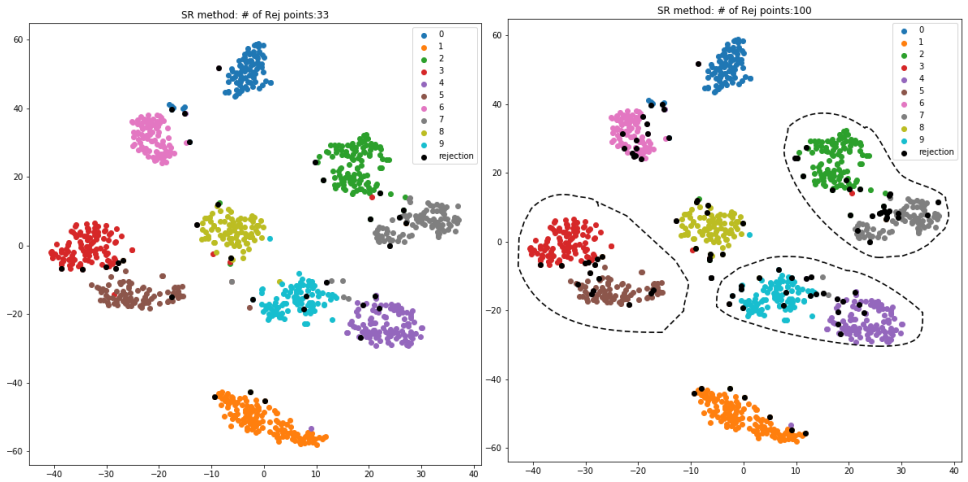

(a) h set to reject 30 points (b) h set to reject 100 points

Figure 11: t-SNE plot of a regular deep model with different h.

11.3 t-SNE Plots

The experiment is done on MNIST with a 4-layer CNN model trained until convergence (10 epochs). The t-SNE (we used sklearn and its default parameters) plot is based on the output of the second-to-last layer. The raw t-SNE of the two models are in Figure 10. The points rejected by SR on the simple model is given in Figure 11 and that by a deep gambler model is in Figure 12. We see the the normal model has not learned a representation that is easily separable (circled clusters), while a deep gambler model learned a representation with a large margin, which is often associated with superior performance [11, 28, 17]. From the plot, we notice that the baseline model seems to have mixed up 4 with 9, 3 with 5, and 2 with 7. More interestingly, we also note that we can also use the SR method on a deep gambler model, and we notice that in this case the rejected points are almost always the same. Suggesting that the reason for our superior performance is due to learning a better representation.

(a) h set to reject 30 points (b) h set to reject 100 points

Figure 12: t-SNE plot of a deep gambler model with different h.